nature plants

ARTICLES

https://doi.org/10.1038/s41477-020-0740-1

Stimulating photosynthetic processes increases productivity and water-use efficiency in the field

Patricia E. López-Calcagno[1,3]✉, Kenny L. Brown[1,3], Andrew J. Simkin[1,2,3], Stuart J. Fisk[1], Silvere Vialet-Chabrand[1], Tracy Lawson[1] and Christine A. Raines[1]✉

Previous studies have demonstrated that the independent stimulation of either electron transport or RuBP regeneration can increase the rate of photosynthetic carbon assimilation and plant biomass. In this paper, we present evidence that a multigene approach to simultaneously manipulate these two processes provides a further stimulation of photosynthesis. We report on the introduction of the cyanobacterial bifunctional enzyme fructose-1,6-bisphosphatase/sedoheptulose-1,7-bisphosphatase or the overexpression of the plant enzyme sedoheptulose-1,7-bisphosphatase, together with the expression of the red algal protein cytochrome c_6, and show that a further increase in biomass accumulation under both glasshouse and field conditions can be achieved. Furthermore, we provide evidence that the stimulation of both electron transport and RuBP regeneration can lead to enhanced intrinsic water-use efficiency under field conditions.

The yield potential of seed crops grown under optimal management practices, and in the absence of biotic and abiotic stress, is determined by incident solar radiation over the growing season, the efficiency of light interception, energy conversion efficiency and the partitioning or harvest index. For the major crops, the only component not close to the theoretical maximum is energy conversion efficiency, which is determined by gross canopy photosynthesis minus respiration. Photosynthesis is therefore a target for improvement to raise the yield potential in major seed crops[1–3].

Transgenic experiments and modelling studies have provided compelling evidence that increasing the levels of photosynthetic enzymes in the Calvin–Benson (CB) cycle has the potential to impact photosynthetic rate and yield[1,2,4–15]. The overexpression of SBPase in tobacco[5,7,8], *Arabidopsis*[9], tomato[15] and wheat[16] has demonstrated the potential of manipulating the expression of CB cycle enzymes and specifically the regeneration of RuBP to increase growth, biomass (30–42%) and even seed yield (10–53%). Similarly, the overexpression of other enzymes, including FBPA[14], cyanobacterial SBPase, FBPase[17] and the bifunctional fructose-1,6-bisphosphatases/sedoheptulose-1,7-bisphosphatase (FBP/SBPase[4,18,19]), in a range of species has shown that increasing photosynthesis increases yield. In addition to the manipulation of CB cycle genes, increasing photosynthetic electron transport has been shown to have a beneficial effect on plant growth. The overexpression of the Rieske FeS protein (a key component of the cytochrome b_6f complex) in *Arabidopsis* has previously been shown to lead to increases in electron transport rates, CO_2 assimilation, biomass and seed yield[20]. Similar results were also observed when the Rieske FeS protein was overexpressed in the C_4 plant *Setaria viridis*, demonstrating that this manipulation has the potential to have a positive effect in both C_3 and C_4 species[21]. Furthermore, the introduction of the algal cytochrome c_6 protein into *Arabidopsis* and tobacco resulted in increased growth[22,23]. In transgenic plants expressing cytochrome c_6, the electron transport rate was increased, along with ATP, NADPH, chlorophyll, starch content and capacity for CO_2 assimilation. Higher plants have been proposed to have lost the cytochrome c_6 protein through evolution, but in green algae and cyanobacteria, which have genes for both cytochrome c_6 and plastocyanin (PC), cytochrome c_6 has been shown to replace PC as the electron transporter connecting the cytochrome b_6f complex with photosystem I (PSI) under Cu deficiency conditions[24,25]. There is evidence showing that PC can limit electron transfer between the cytochrome b_6f complex and PSI[26], and in *Arabidopsis*, it has been shown that introduced algal cytochrome c_6 is a more efficient electron donor to P700 than PC[22]. This evidence suggests that the introduction of the cytochrome c_6 protein in higher plants is a viable strategy for improving photosynthesis.

This paper aims to test the hypothesis that combining an increase in the activity of a CB cycle enzyme (specifically, enhancing RuBP regeneration) with the stimulation of the electron transport chain can boost photosynthesis and yield above that observed when these processes are targeted individually. *Nicotiana tabacum* plants expressing the algal cytochrome c_6 and either the cyanobacterial FBP/SBPase or the higher plant SBPase were generated using two different tobacco cultivars. The analysis presented here demonstrates that the simultaneous stimulation of electron transport and RuBP regeneration leads to a notable increase in photosynthetic carbon assimilation, and results in increased biomass and yield under both glasshouse and field conditions.

Production and selection of tobacco transformants

Previous differences observed in the biomass accumulation between *Arabidopsis* and tobacco overexpressing SBPase and SBPase plus FBPA[8,9] led us to explore the effects of similar manipulations (RuBP regeneration by the overexpression of SBPase or the introduction of the cyanobacterial FBP/SBPase, together with enhanced electron transport) in two different tobacco cultivars with different growth habits: *N. tabacum* cv. Petit Havana, with indeterminate growth, and *N. tabacum* cv. Samsun, with determinate growth. Sixty lines of cv. Petit Havana and up to fourteen lines of cv. Samsun were generated per construct, and T0 and T1 transgenic tobacco were screened by quantitative PCR (qPCR) and immunoblot analysis to select independent lines with expression of the transgenes (data not shown).

[1]School of Life Sciences, University of Essex, Colchester, UK. [2]Genetics, Genomics and Breeding, NIAB EMR, East Malling, UK. [3]These authors contributed equally: Patricia E. López-Calcagno, Kenny L. Brown, Andrew J. Simkin. ✉e-mail: pelope@essex.ac.uk; rainc@essex.ac.uk

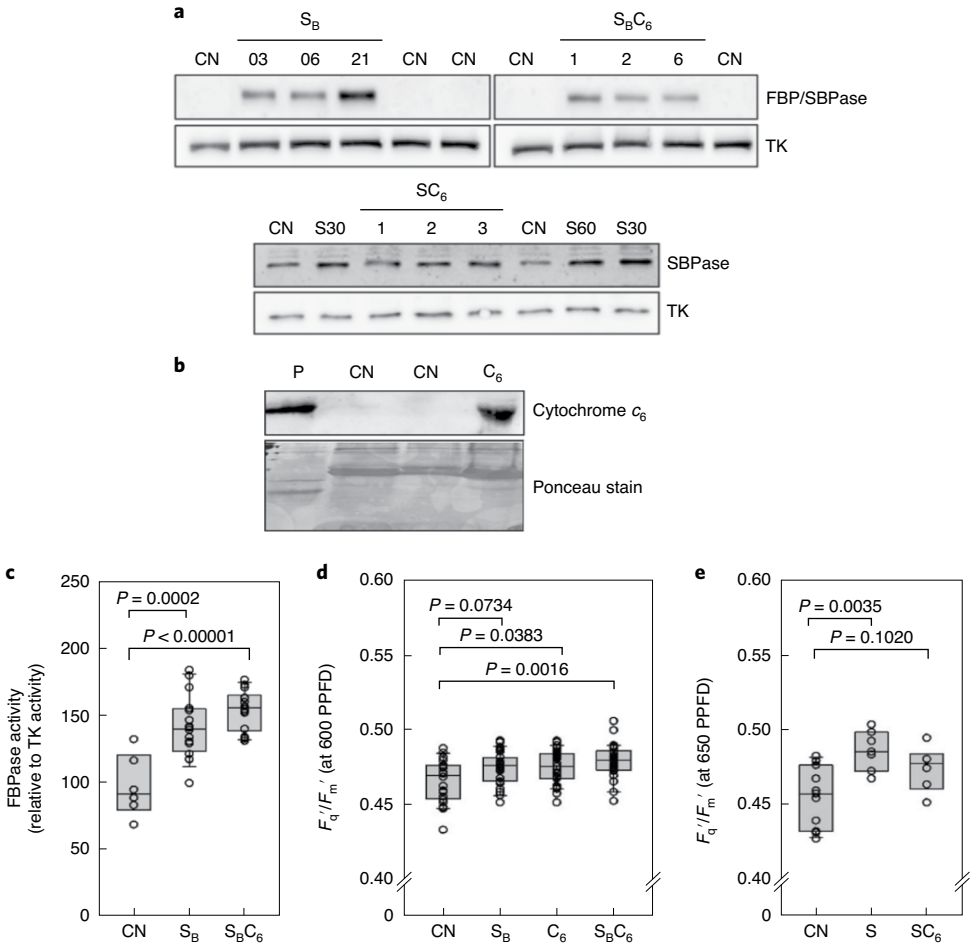

Fig. 1 | Screening of transgenic plants overexpressing FBP/SBPase, SBPase and cytochrome c_6. **a**, Immunoblot analysis of protein extracts from mature leaves of the evaluated S_B, S_BC_6, S and SC_6 lines compared with WT and azygous (CN) plants, using FBP/SBPase and SBPase antibodies. Equal amounts of protein were loaded; transketolase (TK) is the loading control. The analysis was repeated three times, with similar results. **b**, Immunoblot analysis of cytochrome c_6 protein extract from mature leaves of C_6 compared with CN plants. Ponceau staining was used as a loading control for the plant samples only. Additionally, a crude *Porphyra* sp. protein extract (P) is presented as confirmation of the correct band size for the introduced cytochrome c_6. The analysis was repeated three times, with similar results. **c**, FBPase activity in S_B ($n=16$) and S_BC_6 ($n=14$) relative to CN ($n=6$) plants. **d**,**e**, Chlorophyll fluorescence imaging of plants grown in controlled environmental conditions was used to determine F_q'/F_m' at 600–650 μmol m^{-2} s^{-1}, 14 to 21 d after sowing. The values for CN ($n=20$), S_B ($n=28$), C_6 ($n=29$) and S_BC_6 ($n=30$) are shown in **d**; those for CN ($n=11$), S ($n=7$) and SC_6 ($n=6$) are shown in **e**. The box plots show the median (central line), the lower and upper quartiles (box) and the minimum and maximum values (whiskers). The statistical tests used include ANOVA and post-hoc Tukey tests. PPFD, photosynthetic photon flux density.

N. tabacum cv. Petit Havana T2/T3 progeny expressing FBP/SBPase (S_B, lines S_B03, S_B06, S_B21 and S_B44) or cytochrome c_6 (C_6, lines C15, C41, C47 and C50) and cv. Samsun lines expressing SBPase and cytochrome c_6 (SC_6, lines SC1, SC2 and SC3) were produced by agrobacterium transformation. *N. tabacum* cv. Petit Havana plants expressing both S_B and C_6 were generated by crossing S_B lines (S_B06, S_B21 and S_B44) with C_6 lines (C15, C47 and C50) to generate four independent S_BC_6 lines: S_BC1 ($S_B06 \times C47$), S_BC2 ($S_B06 \times C50$), S_BC3 ($S_B44 \times C47$) and S_BC6 ($S_B21 \times C15$). Semiquantitative PCR with reverse transcription (RT–PCR) was used to detect the presence of the FBP/SBPase transcript in lines S_B and S_BC_6; cytochrome c_6 in lines C_6, S_BC_6 and SC_6; and SBPase in lines S and SC_6 (Supplementary Fig. 1). The selected S_B and S_BC_6 lines were shown to accumulate FBP/SBPase protein, and S and SC_6 were shown to overexpress the SBPase protein by immunoblot analysis (Fig. 1a and Supplementary Fig. 2). In addition to immunoblot analysis, we analysed the total extractable FBPase activity in the leaves of the cv. Petit Havana T2/T3 and F3 homozygous progeny lines used to determine chlorophyll fluorescence and photosynthetic parameters. This analysis showed that these plants (S_B and S_BC_6) had increased levels of FBPase activity ranging from 34 to 47% more than the control (CN) plants (Fig. 1c). The full set of assays showing the variation in FBPase activities between plants can be seen in Supplementary Fig. 3. The S and SC_6 lines were from the same generation of transgenic plants used in a previous study and shown to have increased SBPase activity[8]. The cytochrome c_6 antibody (raised against a peptide from the *Porphyra umbilicalis* protein) was unable to detect less than 60 ng of purified cytochrome c_6 protein extracted from *Escherichia coli* (Supplementary Fig. 4), and the immunoblotting of leaf extracts did not result in a signal. However, a band of the expected molecular weight was identified in semipurified extracts from lines C15, C41 and C47, providing qualitative confirmation of the presence of cytochrome c_6 in the transgenic tobacco plants (Fig. 1b and Supplementary Fig. 5a). No bands were observed in semipurified extracts from CN plants. To provide further evidence of the presence of introduced cytochrome c_6 protein, a spectral scan was run using the semipurified protein extracts of C_6 and CN plants; the Soret peak at 420 nm

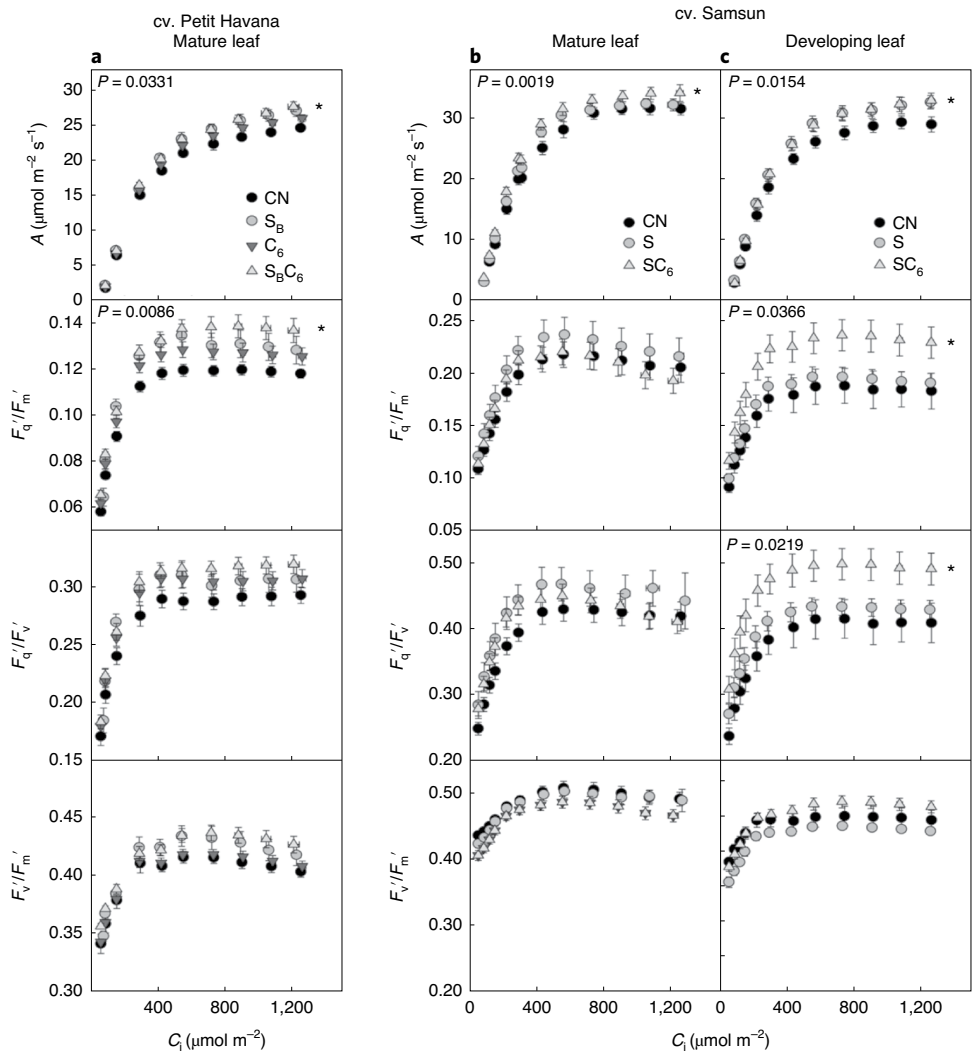

Fig. 2 | Photosynthetic responses of transgenic plants grown in the glasshouse. a–c, A, F_q'/F_m', F_q'/F_v' and F_v'/F_m' are presented for mature leaves of CN ($n=10$), S_B ($n=7$), C_6 ($n=11$) and S_BC_6 ($n=9$) plants (cv. Petit Havana) (**a**), and for mature leaves of CN ($n=10$), S ($n=8$) and SC_6 ($n=10$) (**b**) and developing leaves of CN ($n=6$), S ($n=6$), SC_6 ($n=9$) plants (cv. Samsun) (**c**). The parameters were determined as functions of increasing CO_2 concentrations at saturating-light levels in developing (11–13 cm in length) and mature leaves. The plants were grown in the glasshouse, where light levels oscillated between 400 and 1,000 μmol m^{-2} s^{-1} (supplemental light ensured a minimum of 400 μmol m^{-2} s^{-1}). The CN group represents both WT and azygous plants. The asterisks indicate significant differences between the transgenics and CN plants, using a linear mixed-effects model and type III ANOVA and contrast analysis. *$P<0.05$. The exact P value is indicated in each plot.

demonstrated the presence of the heme group and was detectable only in the C_6 transgenic plants and not in the CN plants (Supplementary Fig. 5b). Additionally, a physiological assay probing the response of photosynthesis during light induction was performed. CN and C_6 plants were provided with saturating light and CO_2 concentrations after a period of darkness. The C_6 plants were shown to have both a more rapid response and a greater rate of net CO_2 assimilation (A) than the CN plants (Supplementary Fig. 6a,d). The faster increase in A was accompanied by a quicker rise in the operating efficiency of both photosystem II (PSII) (F_q'/F_m') and PSI (YI), providing evidence that electron flow through both photosystems was increased in these plants. This increase in electron transport could contribute to the higher A values observed by providing the required energy (ATP) and reductant (NADPH). This response was further accelerated in S_BC_6 transgenic plants, probably due to the increased sink capacity provided by CB cycle activity (Supplementary Fig. 6).

Chlorophyll fluorescence analysis confirmed that in young plants, the operating efficiency of PSII photochemistry (F_q'/F_m') at an irradiance of 600–650 μmol m^{-2} s^{-1} was significantly higher in all selected lines than the CN plants which includes both wild-type (WT) and azygous plants (Fig. 1d,e). However, the F_q'/F_m' values of the S_BC_6 and SC_6 lines were not significantly different from the F_q'/F_m' values obtained from the plants individually expressing FBP/SBPase (S_B), cytochrome c_6 (C_6) or SBPase (S).

Stimulation of electron transport and RuBP regeneration increases photosynthesis

Transgenic lines selected on the basis of the initial screens described above were grown in the glasshouse, in natural light supplemented to provide illumination between 400 and 1,000 μmol m^{-2} s^{-1}. The values of A and F_q'/F_m' were determined as functions of the internal CO_2 concentration (C_i) in mature and developing leaves of *N. tabacum* cv. Samsun (S and SC_6) and in mature leaves of

Table 1 | J_{max}, Vc_{max} and A_{max} of WT and transgenic lines

	A/C_i				
Cultivar	**Leaf stage**	**Line**	**Vc_{max} (μmol m^{-2} s^{-1})**	**J_{max} (μmol m^{-2} s^{-1})**	**A_{max} (μmol m^{-2} s^{-1})**
Samsun	Developing	CN	72.32 ± 5.5	157.51 ± 6.0	29.6 ± 1.1
		S	87.7 ± 4.3	**179.8 ± 4.9***	**34.1 ± 0.7***
		SC_6	86.5 ± 3.5	**181.2 ± 3.6***	**33.7 ± 1.1***
	Mature	CN	77.2 ± 3.3	171.0 ± 6.0	31.6 ± 1.0
		S	81.3 ± 6.1	183.5 ± 9.0	32.2 ± 0.7
		SC_6	90.3 ± 3.3	193.1 ± 5.4	**34.9 ± 1.1***
Petit Havana	Mature	CN	69.6 ± 2.0	121.5 ± 1.3	24.6 ± 0.5
		S_B	69.0 ± 5.1	128.7 ± 3.8	27.0 ± 0.8
		C_6	79.3 ± 7.0	129.9 ± 5.1	25.6 ± 0.5
		S_BC_6	76.5 ± 4.2	132.0 ± 3.8	**27.4 ± 0.8***

The results were determined from the A/C_i curves in Fig. 2 using the equations published by von Caemmerer and Farquhar[55]. Significant differences are shown in boldface (*$P < 0.05$). Samsun mature leaves, CN ($n = 10$), S ($n = 8$), SC_6 ($n = 10$); Samsun developing leaves, CN ($n = 6$), S ($n = 6$), SC_6 ($n = 9$); Petit Havana leaves, CN ($n = 10$), S_B ($n = 7$), C_6 ($n = 11$), S_BC_6 ($n = 9$). The mean and s.e.m. are shown.

N. tabacum cv. Petit Havana (S_B, C_6 and S_BC_6) (Fig. 2). The transgenic plants displayed greater CO_2 assimilation rates than those of the CN plants. *A* was 15% higher in the mature leaves of the SC_6 plants than in the CN plants at a C_i of approximately 300 μmol mol^{-1} (the C_i prevailing at the current atmospheric CO_2 concentration) (Fig. 2b). The developing leaves of the SC_6 plants also showed significant increases in F_q'/F_m' and in the PSII efficiency factor (F_q'/F_v', which is determined by the ability of the photosynthetic apparatus to maintain Q_A in the oxidized state and therefore a measure of photochemical quenching) when compared with the CN plants (Fig. 2c). Interestingly, in mature leaves of the cv. Samsun transgenic plants, the differences in assimilation rates and in the operating efficiency of PSII photochemistry between the transgenic and the CN plants were smaller than in the developing leaves. Only the S transgenic plants displayed higher average values of F_q'/F_m' and F_q'/F_v' than the CN plants at all CO_2 concentrations measured. In contrast, the mature leaves of SC_6 plants displayed F_q'/F_v' values higher than the CN only at C_i levels between 300 and 900 μmol mol^{-1} (Fig. 2b).

Similar trends were shown for the *N. tabacum* cv. Petit Havana transgenic plants, which displayed higher average values of *A* and F_q'/F_m' than the CN (Fig. 2a). In the leaves of the S_BC_6 plants (cv. Petit Havana), these significant increases were similar to those in the developing leaves of the SC_6 lines (cv. Samsun). No significant differences in PSII maximum efficiency (F_v'/F_m') were observed between the CN and the transgenics in either cultivar.

The developing leaves of both the S and SC_6 plants (cv. Samsun) showed significant increases in both the maximum electron transport and RuBP regeneration rate (J_{max}) and the maximum assimilation (A_{max}) when compared with the CN plants (Table 1). The mature leaves of the SC_6 (cv. Samsun) and S_BC_6 (cv. Petit Havana) transgenics also displayed significantly higher values of A_{max} than the CN, and higher average values for the maximum carboxylation rate of Rubisco (Vc_{max}) and J_{max} were also evident in these leaves. These results show that the simultaneous stimulation of electron transport and RuBP regeneration by the expression of cytochrome c_6 in combination with FBP/SBPase or SBPase has a greater impact on photosynthesis than the single manipulations in all plants analysed.

Stimulation of electron transport and RuBP regeneration improves growth

In parallel experiments, plants expressing FBP/SBPase (S_B), cytochrome c_6 (C_6) and both (S_BC_6) (*N. tabacum* cv. Petit Havana) and plants expressing SBPase (S) and SBPase with cytochrome c_6 (SC_6) (*N. tabacum* cv. Samsun) were grown in the glasshouse for four and six weeks, respectively, before harvesting. The height, leaf number, total leaf area and above-ground biomass were determined for each plant (Fig. 3 and Supplementary Fig. 7). All of the transgenic plants analysed here displayed increased height compared with CN plants. Plants expressing cytochrome c_6 (C_6, S_BC_6 (cv. Petit Havana) and SC_6 (cv. Samsun)) had significant increases in leaf area and in stem and leaf biomass compared with their respective CNs (Fig. 3 and Supplementary Figs. 8 and 9). In the S_B transgenic plants (cv. Petit Havana), only the biomass of the stem was greater than in the CN plants. Notably, the S_BC_6 and SC_6 transgenics displayed significantly greater leaf area than the single S_B and S transgenic plants, respectively. The total increase in above-ground biomass when compared with the CN group was 35% in S_B, 44% in C_6 and 9% in S, with consistently higher means in the double manipulations S_BC_6 (52%) and SC_6 (32%) (Fig. 3).

Expression of FBP/SBPase and cytochrome c_6 increases growth and water-use efficiency

To test whether the increases in biomass observed in these transgenic plants under glasshouse conditions could be reproduced in a field environment, a subset of lines was selected for testing in the field. Since the larger percentage increases in biomass were displayed by the manipulations in *N. tabacum* cv. Petit Havana, these plants were selected and tested in three field experiments in two different years (2016 and 2017).

In 2016, a small-scale replicated control experiment was carried out to evaluate vegetative growth in the field, in the lines expressing single gene constructs for FBP/SBPase (S_B) and cytochrome c_6 (C_6) (Supplementary Fig. 14a). The plants were germinated and grown under controlled-environment conditions for 25 d before being moved to the field. After 14 d in the field, the plants were harvested at an early vegetative stage, and plant height, total leaf area and above-ground biomass were measured (Fig. 4a–c and Supplementary Fig. 10a). These data revealed that the S_B and C_6 plants showed increases in height, leaf area and above-ground biomass of 27%, 35% and 25%, respectively, for S_B and 50%, 41% and 36%, respectively, for C_6 when compared with CN plants.

In 2017, two larger-scale, randomized block design field experiments were carried out to evaluate performance in the S_B, C_6 and S_BC_6 plants compared with CN plants (Supplementary Fig. 14b). The plants were grown from seed in the glasshouse for 33 d and were then moved to the field and allowed to grow until the onset of flowering (another 24–33 d) before harvesting. In Fig. 4d–i, it can be seen that the S_B and C_6 plants harvested after the onset of flowering did not display any significant increases in height, leaf area or

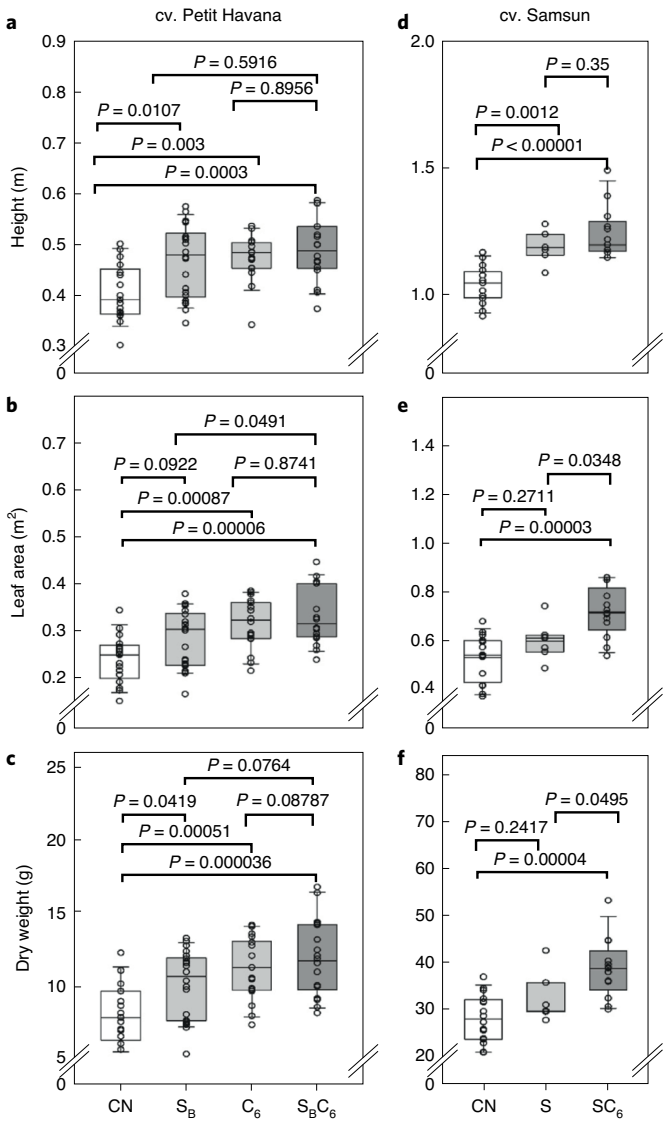

Fig. 3 | Increased SBPase or expression of FBP/SBPase and cytochrome c_6 increases biomass in glasshouse-grown plants. a–f, Tobacco plants were germinated in growth cabinets and moved to the glasshouse at 10–14 d post-germination. Forty-day-old (cv. Petit Havana) or fifty-six-day-old (cv. Samsun) plants were harvested, and plant height (**a**,**d**), leaf area (**b**,**e**) and above-ground biomass (dry weight) (**c**,**f**) were determined. The CN group represents both WT and azygous plants. The values for cv. Petit Havana CN ($n=17$), S_B ($n=21$), C_6 ($n=18$) and S_BC_6 ($n=18$) are shown in **a**–**c**; those for cv. Samsun CN ($n=16$), S ($n=7$) and SC_6 ($n=13$) are shown in **d**–**f**. The box plots show the median (central line), the lower and upper quartiles (box) and the minimum and maximum values (whiskers). The statistical analysis was done using ANOVA with post-hoc Tukey tests.

biomass when compared with the CN plants. Interestingly, plants expressing both FBP/SBPase and cytochrome c_6 (S_BC_6) displayed significant increases in a number of growth parameters, with 13%, 17% and 27% increases in height, leaf area and above-ground biomass, respectively, when compared with the CN plants.

Additionally, in the 2017 field experiments, A as a function of C_i at saturating light (A/C_i) was determined. In 2017 experiment 1, a significant increase in A was observed in S_B and C_6 plants without differences in F_q'/F_m' (Fig. 5a). However, in 2017 experiment 2, no differences in A or in F_q'/F_m' values were evident in the C_6 and S_BC_6 plants when compared with the CN plants (Fig. 5b). An analysis of A as a function of light (A/Q) showed either small or no significant differences in A between genotypes (Fig. 6a and Supplementary Fig. 11a). Interestingly, stomatal conductance (g_s) in the S_BC_6 plants was significantly lower than in the C_6 and CN plants at light intensities above 1,000 µmol m^{-2} s^{-1} (Fig. 6b), resulting in a significant increase in intrinsic water-use efficiency (iWUE) for S_BC_6 plants (Fig. 6d). No significant differences in iWUE were observed for S_B or C_6 transgenic plants (Fig. 6d and Supplementary Fig. 11d).

Discussion

In this study, we describe the generation and analysis of transgenic plants with simultaneous increases in electron transport and improved capacity for RuBP regeneration, in two different tobacco cultivars. Here we have shown that the independent stimulation of electron transport (by the expression of cytochrome c_6) and stimulation of RuBP regeneration (by the expression of FBP/SBPase or overexpression of SBPase) increased photosynthesis and biomass in glasshouse studies. Furthermore, we demonstrated how the targeting of these two processes simultaneously (in the S_BC_6 and SC_6 plants) had an even greater effect in stimulating photosynthesis and growth. Additionally, in field studies we demonstrated that plants with simultaneous stimulation of electron transport and of RuBP regeneration had increased iWUE with increases in biomass.

Under glasshouse conditions, increases in photosynthesis were observed in all of the transgenic plants analysed here, and these increases were found to be correlated with increased biomass. Although increases in photosynthesis and biomass have been reported for plants with stimulation of RuBP regeneration in both model[4,5,7,8,27] and crop[16,18] species and of electron transport in *Arabidopsis* and tobacco[20,22,23], the data presented here provide the first report of increased photosynthesis and biomass by the simultaneous stimulation of electron transport and RuBP regeneration. Increases in A were observed under glasshouse conditions in the leaves of all of the transgenic tobacco plants and in both tobacco cultivars (cv. Petit Havana and cv. Samsun). The analysis of the A/C_i response curves showed that the average values for the photosynthetic parameters Vc_{max}, J_{max} and A_{max} increased by up to 11, 14 and 15%, respectively. These results indicate that not only were the maximal rates of electron transport and RuBP regeneration increased, but also the rate of carboxylation by Rubisco was increased. Although this may seem counterintuitive in that we have not directly targeted Rubisco activity, it is in keeping with a study by Wullschleger[28] of over 100 plant species that showed a linear correlation between J_{max} and Vc_{max}. Furthermore, it has also been shown that the overexpression of SBPase leads not only to a notable increase in J_{max} but also to increases in Vc_{max} and Rubisco activation state[5,8].

Notably, in the greenhouse study, the highest photosynthetic rates were observed in plants in which both electron transport and RuBP regeneration (S_BC_6 and SC_6) were boosted, suggesting that the coexpression of these genes results in an additive effect on improving photosynthesis. In addition to the increases in A, the plants with simultaneous stimulation of electron transport and RuBP regeneration displayed a significant increase in F_q'/F_m', indicating a higher quantum yield of linear electron flux through PSII compared with the CN plants. These results are in keeping with the published data for the introduction of cytochrome c_6 and the overexpression of the Rieske FeS protein in *Arabidopsis*[20,22]. In these studies, the plants had a higher quantum yield of PSII and a more oxidized plastoquinone pool[22], suggesting that, although PC is not always limiting under all growth conditions[29], there is scope to stimulate the reduction of PSI by using alternative, more efficient electron donors to PSI such as cytochrome c_6 (refs. [22,26]). Furthermore, in the S_BC_6 and SC_6 plants, the increase in F_q'/F_m' was found to be driven largely by the increase in F_q'/F_v'. This suggests that the increase in efficiency in these plants is probably due to the stimulation of processes downstream of PSII, such as CO_2 assimilation.

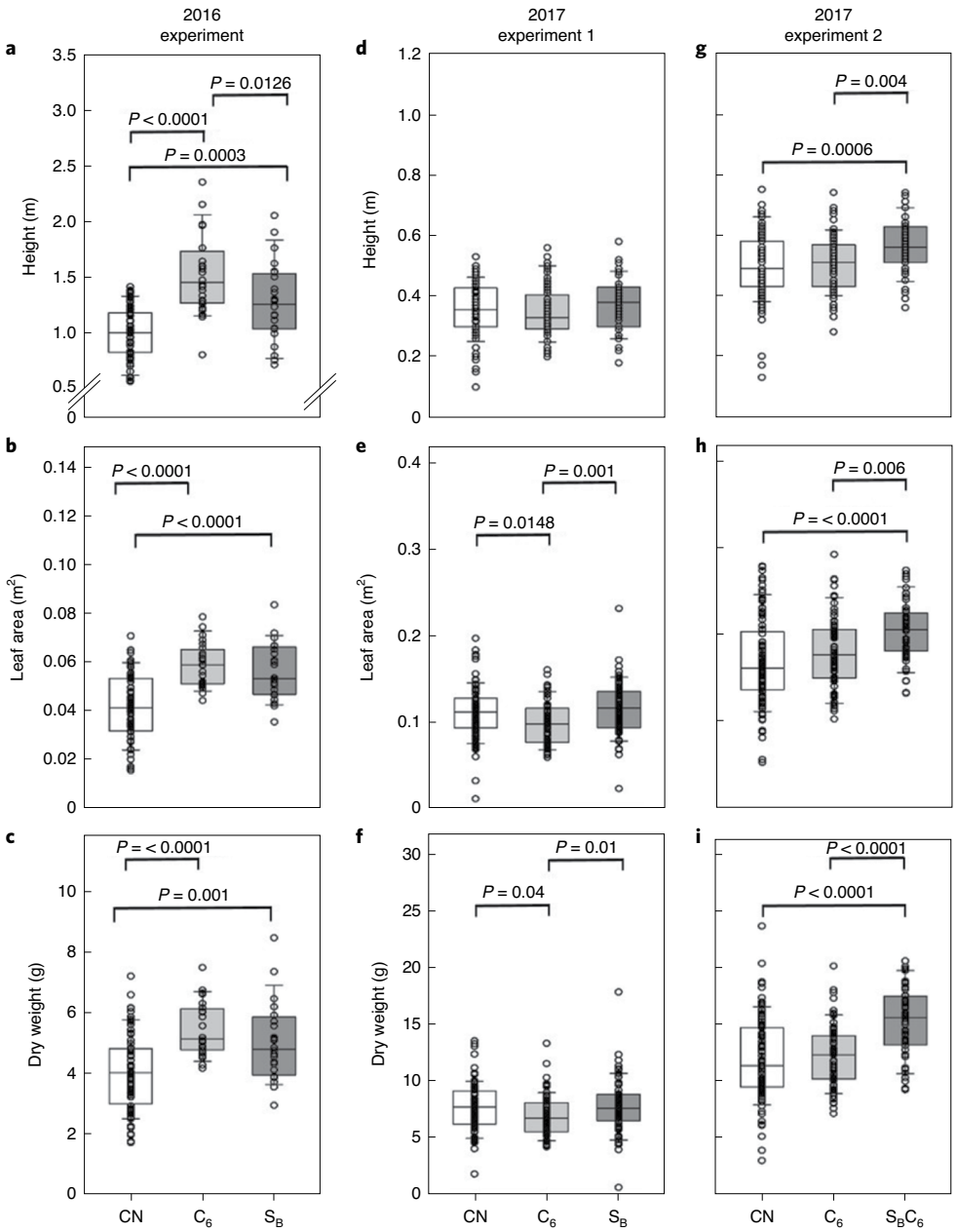

Fig. 4 | Simultaneous expression of FBP/SBPase and cytochrome c_6 increases biomass in field-grown plants. a–c, Forty-day-old (young) 2016 field-grown plants (the plants were germinated and grown in glasshouse conditions for 26 d and then allowed to grow in the field in summer 2016 for 14 d). **d–i**, Fifty-seven-day-old (experiment 1) or sixty-one-day-old (experiment 2) (flowering) 2017 field-grown plants (the plants were germinated and grown in glasshouse conditions for 26 d and grown in the field in summer 2017 until flowering established, circa 30 d). Plant height (**a**,**d**,**g**), leaf area (**b**,**e**,**h**) and total above-ground biomass (dry weight) (**c**,**f**,**i**) are shown. The sample sizes are as follows: in **a–c**, CN ($n = 72$), S_B ($n = 33$) and C_6 ($n = 33$); in **d–f**, CN ($n = 93$), S_B ($n = 71$) and C_6 ($n = 70$); in **g–i**, CN ($n = 97$), C_6 ($n = 72$) and S_BC_6 ($n = 47$). The box plots show the median (central line), the lower and upper quartiles (box) and the minimum and maximum values (whiskers). The statistical analysis was done using ANOVA with post-hoc Tukey tests.

To provide further evidence of the applicability of targeting both electron transport and RuBP regeneration to improve crop yields, we tested these plants in the field. Here we showed that the expression of FBP/SBPase alone led to increases in growth and biomass in the 2016 field-grown plants of 22–40%, when they were harvested during early vegetative growth, before the onset of flowing. Interestingly, when these plants were harvested later in development (after the onset of flowering), in the 2017 field trials, this advantage was no longer evident, and the single FBP/SBPase expressors were indistinguishable from the CN plants. These results are in contrast to the 2016 field data and may be due to the later timing of the harvest in the 2017 experiments. The transgenic plants expressing cytochrome c_6 alone also showed enhanced growth and biomass in early development, but as with the FBPase/SBPase plants, this improvement was no longer evident when the plants were harvested after flowering. This difference in biomass gain between the early and late harvests was not observed in a parallel experiment, where the overexpression of H-protein was shown to increase biomass under field conditions in plants harvested in early development and after the onset of flowering[30]. These results suggest that the expression of FBP/SBPase or cytochrome c_6 alone may provide an advantage under particular sets of conditions or at specific stages of plant

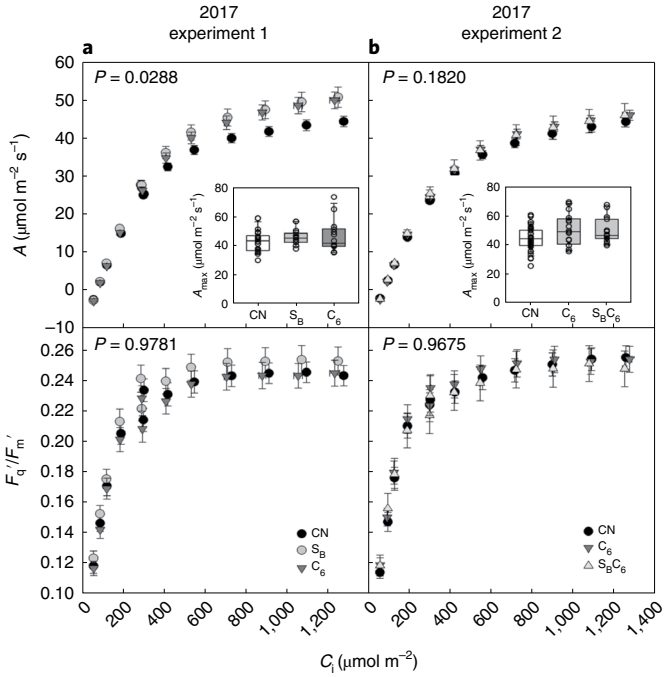

Fig. 5 | Photosynthetic capacity of field-grown transgenic plants. **a**,**b**, Photosynthetic carbon fixation rates and operating efficiency of PSII as functions of increasing CO_2 concentrations at saturating-light levels in mature leaves from CN and transgenic plants. The sample sizes are as follows: in **a**, CN ($n=21$), S_B ($n=16$) and C_6 ($n=16$); in **b**, CN ($n=22$), C_6 ($n=16$) and S_BC_6 ($n=14$). The CN group represents both WT and azygous plants. The mean and s.e.m. are presented. The inset box plots show the median (central line), the lower and upper quartiles (box) and the minimum and maximum values (whiskers). A linear mixed-effects model and type III ANOVA were applied. The exact *P* value is indicated in each plot.

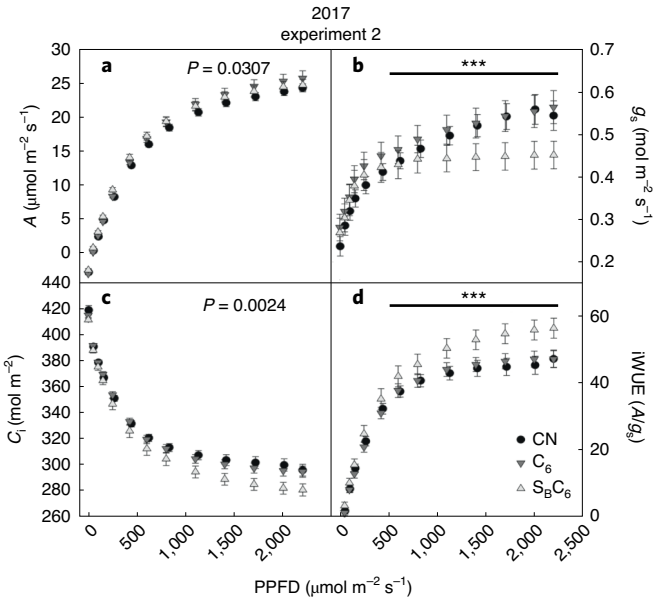

Fig. 6 | Simultaneous expression of FBP/SBPase and cytochrome c_6 can increase water-use efficiency under field conditions. a–d, *A* (**a**), g_s (**b**), C_i (**c**) and iWUE (**d**) as functions of light (PPFD) in field-grown plants. CN $n=22$, C_6 $n=16$, S_BC_6 $n=14$. A linear mixed-effects model and type III ANOVA were applied. The exact *P* value is indicated in each plot.

development. This might be exploitable for some crops where an early harvest is desirable (such as some types of lettuce, spinach and tender greens)[18]. In contrast to the results with the single manipulations described above, plants expressing both cytochrome c_6 and FBP/SBPase displayed a consistent increase in biomass after flowering under field conditions.

In the transgenic lines grown in the field, the correlations between increased photosynthesis and increased biomass were less consistent than those observed under glasshouse conditions. The significant increases in photosynthetic capacity displayed by the FBP/SBPase and cytochrome c_6 expressors in 2017 experiment 1 provided clear evidence that these individual manipulations are able to stimulate photosynthetic performance under field conditions. However, no increase in biomass was evident in these plants. In contrast, in 2017 experiment 2, we did not detect any significant differences in photosynthetic capacity in either the cytochrome c_6 expressors or the plants with the simultaneous expression of FBP/SBPase and cytochrome c_6, but increased biomass was evident. At this point, we have no explanation for this disparity. However, although not significantly different, in all experiments, the mean *A* values of the transgenic plants were consistently higher than those of the CN plants. It is known that even small increases in assimilation throughout the lifetime of a plant will have a cumulative effect, which could translate into a substantial biomass accumulation[8]; this may partly explain the disparity in the biomass results presented. Furthermore, the phenotyping experiments carried out on C_6 and S_BC_6 plants (Supplementary Fig. 6) showed that there was a more rapid induction of photosynthesis, particularly in S_BC_6 plants. This characteristic might also contribute to an increase in photosynthetic rates and biomass when plants are grown in fluctuating light conditions, but would not be detectable in the steady-state measurements performed in our field experiments.

An unexpected result that was found in the plants with the simultaneous expression of FBP/SBPase and cytochrome c_6 (S_BC_6) is that these plants had a lower g_s and lower C_i at light intensities above 1,000 μmol m^{-2} s^{-1}, when compared with the CN plants. Normally, lower C_i would be expected to lead to a reduction in photosynthesis, but the S_BC_6 plants were able to maintain CO_2 assimilation rates equal to or higher than those of CN plants, resulting in an improvement in iWUE. A similar improvement in iWUE was seen in plants overexpressing the NPQ-related protein PsbS[31]. It was shown that light-induced stomatal opening was reduced in these plants, in which a more oxidized Q_A pool was found, and this has been proposed to act as a signal in stomatal movement[32]. In field studies, a higher productivity has been reported for transgenic lines with increased RuBP regeneration than for CN plants when the plants were grown under CO_2 enrichment[7,18]. This fact combined with the higher iWUE discussed above highlights the potential of manipulating electron transport and RuBP regeneration in the development of new varieties able to sustain photosynthesis and yields under climate change scenarios.

Methods

Generation of constructs and transgenic plants. The constructs were generated using Golden Gate cloning[33,34] or Gateway cloning technology[35]. The transgenes were under the control of CaMV35S and FMV constitutive promoters. The construct details are given below and in Supplementary Fig. 12.

For *N. tabacum* cv. Petit Havana, the codon-optimized cyanobacterial bifunctional FBP/SBPase (*slr2094 Synechocystis* sp. PCC 7942; ref. [4]) linked to the geraniol synthase transit peptide[36] and the codon-optimized *P. umbilicalis* cytochrome c_6 (AFC39870) with the chlorophyll *a*/*b* binding protein 6 transit peptide from *Arabidopsis* (AT3G54890) were used to generate the Golden Gate[34] overexpression constructs (EC23083 and EC23028) driven by the FMV[37] and CaMV 35S promoters, respectively (Supplementary Fig. 12a).

The cytochrome c_6 from *P. umbilicalis* was selected because it is commonly found on the UK coastline, and it shares over 86% identity with the previously published *P. yeoenzis* and *Ulva fasciata* used by Chida et al.[22] and Yadav et al.[23].

The level of similarity between these proteins and the fact that the functional regions are identical provide confidence that the cytochrome c_6 proteins from these three species function in similar ways (see the alignment in Supplementary Fig. 13). The *P. umbilicalis* cytochrome c_6 was linked to the transit peptide from the light-harvesting complex I chlorophyll *a*/*b* binding protein 6 (AT3G54890) to generate an overexpression construct driven by the CaMV 35S promoter; B2-C6 in the vector pGWB2 (ref. [35]) was used for the *N. tabacum* cv. Samsun transformation (Supplementary Fig. 12b). The recombinant plasmid B2-C6 was introduced into SBPase overexpressing tobacco cv. Samsun[5] using *Agrobacterium tumefaciens* AGL1 via leaf-disc transformation[38]. Primary transformants (39) (T0 generation) were regenerated on MS medium containing kanamycin (100 mg l^{-1}), hygromycin (30 mg l^{-1}) and augmentin (500 mg l^{-1}). Plants expressing the integrated transgenes were screened using RT–PCR (data not shown).

Similarly, the recombinant plasmids EC23083 and EC23028 were introduced into WT tobacco (*N. tabacum*) cv. Petit Havana using *A. tumefaciens* strain LBA4404 via leaf-disc transformation[38], and the shoots were regenerated on MS medium containing hygromycin (20 mg l^{-1}) and cefotaxime (400 mg l^{-1}). Hygromycin-resistant primary transformants (T0 generation) with established root systems were transferred to soil and allowed to self-fertilize.

Between 12 and 60 independent lines were generated per construct, and 3 or 4 lines were taken forward for further analysis. CN plants used in this study were a combination of WT and null segregant plants from the transgenic lines, verified by PCR for non-integration of the transgene.

Plant growth. *Controlled conditions.* WT tobacco plants and T1 progeny resulting from the self-fertilization of transgenic plants were grown to seed in soil (Levington F2, Fisons). Lines of interest were identified by immunoblot and qPCR. For the experiments with cv. Samsun, the null segregants were selected from the transformed lines. For Petit Havana, the null segregants were selected from the S_BC_6 lines. For the experimental study, T2-T4 and F1-F3 progeny seeds were germinated on soil in controlled-environment chambers at an irradiance of 130 µmol photons per m^2 per s, 22 °C, relative humidity of 60%, in a 16 h photoperiod. The plants were transferred to individual 8 cm pots and grown for two weeks at 130 µmol photons per m^2 per s, 22 °C, relative humidity of 60%, in a 16 h photoperiod. The plants were then transferred to 41 pots and cultivated in a controlled-environment glasshouse (16 h photoperiod, 25 °C–30 °C day/20 °C night, with natural light supplemented under low light induced by cloud cover with high-pressure sodium light bulbs, giving 380–1,000 µmol m^{-2} s^{-1} (high light) from the pot level to the top of the plant). The positions of the plants were changed three times a week, and the plants were watered regularly with a nutrient medium[39]. The plants were positioned such that at maturity, a near-to-closed canopy was achieved, and the temperature range was maintained similar to the ambient external environment. Four leaf discs (0.8 cm in diameter) were taken for immunoblot analysis and FBPase activity. These discs were taken from the same areas of the leaf used for photosynthetic measurements, immediately plunged into liquid N_2 and stored at −80 °C.

Field studies. The plants were grown as described in López-Calcagno et al.[30], and with a methodology broadly analogous to that used commercially for this crop. The field site was situated at the University of Illinois Energy Farm (40.11° N, 88.21° W). Two different experimental designs were used in two different years.

2016: Replicated control design (Supplementary Fig. 14a). The plants were grown in rows spaced 30 cm apart, with the outer boundary being a WT border. The entire experiment was surrounded by two rows of WT borders. The plants were irrigated when required using rain towers. T2 seed was germinated, and after 11 d the plants were moved to individual pots (350 ml). The seedlings were grown in the glasshouse for another 15 d before being moved into the field, and allowed to grow in the field for 14 d before harvest.

2017: Two experiments were carried out two weeks apart. A blocks-within-rows design was used (Supplementary Fig. 14b), in which one block holds one line of each of the five manipulations and each row has all lines. The central 20 plants of each block are divided into five rows of four plants per genotype. Experiment 1 contained CNs (WT and null segregants), FBP/SBPase expressing lines (S_B) and cytochrome c_6 expressing lines (C_6). Experiment 2 contained CNs (WT and null segregants), cytochrome c_6 expressing lines (C_6) and FBP/SBPase and cytochrome c_6 expressing lines (S_BC_6). The seed was germinated, and after 12 d the plants were moved to hydroponic trays (Trans-plant Tray GP009 6912 cells; Speedling Inc.); they were grown in the glasshouse for 20 d before being moved to the field. The plants were allowed to grow in the field until flowering (approximately 30 d) before harvest.

The field was prepared in a similar fashion each year, as described in Kromdijk et al.[40]. Light intensity (LI-quantum sensor; LI-COR) and air temperature (Model 109 temperature probe; Campbell Scientific) were measured nearby on the same field site, and half-hourly averages were logged using a data logger (CR1000; Campbell Scientific).

Complementary DNA generation and RT–PCR. Total RNA was extracted from tobacco leaf discs (sampled from glasshouse-grown plants and quickly frozen in liquid nitrogen) using the NucleoSpin RNA Plant Kit (Macherey-Nagel, Fisher Scientific). The cDNA was synthesized using 1 µg of total RNA in 20 µl using the oligo-dT primer according to the protocol in the RevertAid Reverse Transcriptase kit (Fermentas, Life Sciences). The cDNA was diluted 1 in 4 to a final concentration of 12.5 ng µl^{-1}. For semiquantitative RT–PCR, 2 µl of RT reaction mixture (100 ng of RNA) in a total volume of 25 µl was used with DreamTaq DNA Polymerase (Thermo Fisher Scientific) according to the manufacturer's recommendations. The PCR products were fractionated on 1.0% agarose gels. For qPCR, the SensiFAST SYBR No-ROX Kit was used according to the manufacturer's recommendations (Bioline Reagents Ltd). The primers used for semiquantitative RT–PCR are given in Supplementary Table 1.

Protein extraction and immunoblot analysis. Leaf discs sampled as described above (or fresh *P. umbilicalis* samples) were ground in dry ice, and protein extractions were performed as described in Lopez-Calcagno et al.[41], or using the nucleospin RNA/Protein kit (Macherey-Nagel, http://www.mn-net.com/) during RNA preparations. Protein quantification was performed using the protein quantification kit from Macherey-Nagel. The samples were loaded on an equal protein basis, separated using 12% (w/v) SDS–PAGE, transferred to a nitrocellulose membrane (GE Healthcare Life Science) and probed using antibodies raised against SBPase and FBP/SBPase. Proteins were detected using horseradish peroxidase conjugated to the secondary antibody and ECL chemiluminescence detection reagent (Amersham). The SBPase antibodies have been previously characterized[5,42]. The FBP/SBPase antibodies were raised against a peptide from a conserved region of the protein [C]-DRPRHKELIQEIRNAG-amide, and the cytochrome c_6 antibodies were raised against peptide [C]-[Nle]-PDKTLKKDVLEANS-amide (Cambridge Research Biochemicals). In addition to the aforementioned antibodies, the samples were probed using antibodies raised against transketolase[43,44] as loading controls.

Protein extraction from plants for cytochrome c_6 analysis. Whole leaves were harvested from eight-week-old plants, washed in cold water and then wiped with a cloth soaked in 80% ethanol to remove the majority of leaf residue. The leaves were then washed twice more in cold water, the mid-rib was removed and 50 g of the remaining tissue was placed in a sealed plastic bag and stored overnight in the dark at 4 °C. The proteins were extracted as in Hiyama[45], with a few modifications. The leaf tissue was homogenized in 250 ml of chilled chloroplast preparation buffer (50 mM sodium phosphate buffer, pH 7; 10 mM NaCl) for 30 s. The solution was then filtered through four layers of muslin cloth and centrifuged at 10,000 *g* for 5 min. The resulting pellet was gently resuspended in 50 ml of chilled chloroplast preparation buffer, and the chlorophyll concentration was measured and adjusted to approximately 2 mg ml^{-1}. The resultant mixture was then added to two volumes of preheated (45 °C) solubilization medium (50 mM Tris-HCl, pH 8.8; 3% Triton X), incubated at 45 °C for 30 min and then chilled in an ice bath for a further 30 min before centrifugation at 12,000 *g* for 30 min. The supernatant was stored at −80 °C for use in the next stage. To purify cytochrome c_6 protein, a Biorad Econo-Pac High-Q, 5 ml type wash column was used at a flow rate of 1 ml min^{-1}. First, the column was prepared by washing it with 100 ml of starting buffer (10 mM Tris-HCl, pH 8.8; 0.2% Triton X-100; 20% sucrose). The protein mixture from the previous step was then diluted with an equal volume of chilled starting buffer and passed through the column at a flow rate of 1 ml min^{-1}. Once all the protein was loaded onto the column, it was washed with 1,000 ml of starting buffer supplemented with 10 mM NaCl. Then, 300 ml of starting buffer supplemented with 50 ml NaCl and finally a linear gradient of starting buffer from 50 to 200 mM NaCl over a period of 4 h at 1 ml min^{-1} was performed, and aliquots were collected. For immunoblotting, the samples were acetone precipitated, and the dried protein pellet was then resuspended in 400 µl of solubilization buffer (7 M urea, 2 M thiourea, 50 mM DTT, 4% CHAPS, 0.4% SDS, 5 mM K_2CO_3). Finally, 300 µl of loading buffer was added (50% glycerol, 25% β-mecaptoethanol, 25% EDTA) and the samples heated at 90 °C for 10 min before being loaded on an equal protein basis. The proteins were separated using 18% (w/v) SDS–PAGE, transferred to nitrocellulose membrane and probed using antibodies raised against a cytochrome c_6 peptide. For the identification of the Soret peak, instead of acetone precipitation, the extracts were concentrated by spinning at 8,000 *g* and 4 °C overnight, using a Vivaspin 20 column (GE 28-9323-59), and a spectral scan was done in a SPECTROstar Omega plate reader from BMG Labtech.

Recombinant cytochrome c_6 protein production in *E. coli* and purification. pEC86 plasmids (CCOS accession no. CCOS891) containing *E. coli* cells were transformed with a pET28b plasmid containing the sequence for the mature cytochrome c_6 and grown in kanamycin (50 µg ml^{-1}) and chloramphenicol (35 µg ml^{-1}) containing LB media. IPTG (119 µg ml^{-1}) was added to the culture when OD_{600} reached 0.5–0.6. Five hours later, 330 µl l^{-1} of 1 M ferriprotoporphyrin IX chloride was added to the media, and 24 h post-IPTG, a metal ion master mix (2 mM Ni^{2+}, 2 mM Co^{2+}, 10 mM Zn^{2+}, 10 mM Mn^{2+} and 50 mM Fe^{3+}) was added (1.5 ml l^{-1}). The cells were collected after 5 d of growth and stored at −20 °C. The pellet from 500 ml was resuspended in 3 ml of lysis buffer (50 mM Tris HCl, pH 7.5; 1 mM DTT; 1 mM PMSF), sonicated (11 cycles of 30 s sonication and 30 s rest, at 4 °C) and then spun twice at 10,000 *g* for 20 min at 4 °C. The supernatant was collected and 2 ml loaded in a 124 ml GE Hi Load 16/400 Superdex 75 pg (size exclusion) column. The protein was eluted with 0.05 M Na_2PO_4 pH 7.2, 0.5 M NaCl buffer, at a 1 ml min^{-1} speed, and samples were collected every 5 ml. Fractions collected between 80 and 100 min were concentrated by spinning them at 8,000 *g*

overnight at 4 °C using a Vivaspin 20 (GE 28-9323-59) column. The protein concentration was determined using Bradford quantification, serial dilutions were done with 50 mM Tris HCl pH 7.5 buffer and spectral scans were done in a SPECTROstar Omega plate reader from BMG Labtech, as with the semipurified plant cytochrome c_6 samples.

Determination of FBPase and transketolase activities. FBPase activity was determined by phosphate release as described previously for SBPase with minor modifications[8]. Leaf discs were isolated from the same leaves and frozen in liquid nitrogen after the photosynthesis measurements were completed. The leaf discs were ground to a fine powder in liquid nitrogen and immersed in extraction buffer (50 mM HEPES, pH 8.2; 5 mM MgCl; 1 mM EDTA; 1 mM EGTA; 10% glycerol; 0.1% Triton X-100; 2 mM benzamidine; 2 mM aminocapronic acid; 0.5 mM phenylmethylsulfonylfluoride; 10 mM dithiothreitol), centrifuged for 1 min at 14,000 *g* and 4 °C. The resulting supernatant (1 ml) was desalted through an NAP-10 column (Amersham) and stored in liquid nitrogen. The assay was carried out as descried in Simkin et al.[8]. In brief, 20 µl of extract was added to 80 µl of assay buffer (50 mM Tris, pH 8.2; 15 mM $MgCl_2$; 1.5 mM EDTA; 10 mM DTT; 7.5 mM fructose-1,6-bisphosphate) and incubated at 25 °C for 30 min. The reaction was stopped by the addition of 50 µl of 1 M perchloric acid. Then, 30 µl of samples or standards (PO^{3-}_4 0.125 to 4 nmol) were incubated for 30 min at room temperature after the addition of 300 µl of Biomol Green (Affiniti Research Products), and the A620 was measured using a microplate reader (VERSAmax, Molecular Devices). The activities were normalized to transketolase activity[46]. For the transketolase activity assays, 230 µl of pre-prepared assay mix comprising 14.4 Mm ribose-5-phosphate, 190 µM NADH, 380 µM TPP, 250 U l^{-1} glycerol-3 phosphate dehydrogenase and 6,500 U l^{-1} triose phosphate isomerase was transferred to a 96-well plate (Greiner Bio-One) and placed in a plate reader, which was set at 23 °C for 5 min to stabilize. The plate was then ejected, and 20 µl of each protein sample used for FBPase activity was injected into the wells containing the assay mix. The plate was then read for absorbance at 340 nm every 5 min for 1 h. The activity levels were estimated by subtracting the absorbance value when the reaction becomes linear from the absorbance value 20 to 30 min after the first absorbance reading, depending on the rate of the reaction.

Chlorophyll fluorescence imaging screening in seedlings. Chlorophyll fluorescence imaging was performed on two- to three-week-old tobacco seedlings grown in a controlled-environment chamber at 130 µmol mol^{-2} s^{-1} and ambient (400 µmol mol^{-1}) CO_2. Chlorophyll fluorescence parameters were obtained using a chlorophyll fluorescence imaging system (Technologica[47,48]). The operating efficiency of PSII photochemistry, F_q'/F_m', was calculated from measurements of steady-state fluorescence in the light (F') and maximum fluorescence (F_m') following a saturating 800 ms pulse of 6,300 µmol m^{-2} s^{-1} PPFD and using the following equation: $F_q'/F_m' = (F_m' - F')/F_m'$. Images of F_q'/F_m' were taken under stable PPFD of 600 µmol m^{-2} s^{-1} for Petit Havana and 650 µmol m^{-2} s^{-1} for Samsun[49–51].

Leaf gas exchange. Photosynthetic gas-exchange and chlorophyll fluorescence parameters were recorded using a portable infrared gas analyser (LI-COR 6400; LI-COR) with a 6400-40 fluorometer head unit. Unless stated otherwise, all measurements were taken with a LI-COR 6400 cuvette. Plants grown under glasshouse conditions were maintained at a CO_2 concentration of 400 µmol mol^{-1}, a leaf temperature of 25 °C and a vapour pressure deficit of 1 ± 0.2 kPa. For plants grown under field conditions, the CO_2 concentration was 400 µmol mol^{-1}, the block temperature was set to 2 °C above the ambient temperature (the ambient air temperature was measure before each curve) and the vapour pressure deficit was maintained as close to 1 kPa as possible.

***A*/C_i response curves (photosynthetic capacity).** The response of A to C_i was measured at a saturating light intensity of 2,000 µmol mol^{-2} s^{-1}. Illumination was provided by a red–blue light source attached to the leaf cuvette. Measurements of A were started at the ambient CO_2 concentration (C_a) of 400 µmol mol^{-1}, before C_a was decreased stepwise to a lowest concentration of 50 µmol mol^{-1} and then increased stepwise to an upper concentration of 2,000 µmol mol^{-1}. To calculate A_{max}, Vc_{max} and J_{max}, the C_3 photosynthesis model[52] was fitted to the A/C_i data using a spreadsheet provided by Sharkey et al.[53]. Chlorophyll fluorescence parameters including F_q'/F_m' and the coefficient of photochemical quenching, mathematically identical to F_q'/F_v', were also recorded at each point.

***A*/*Q* response curves.** Photosynthesis as a function of light (A/Q response curves) was measured under the same cuvette conditions as the A/C_i curves mentioned above. The leaves were initially stabilized at a saturating irradiance of 2,200 µmol m^{-2} s^{-1}, after which A and g_s were measured at the following light levels: 2,000, 1,650, 1,300, 1,000, 750, 500, 400, 300, 200, 150, 100, 50 and 0 µmol m^{-2} s^{-1}. The measurements were recorded after A reached a new steady state (1–3 min) and before g_s changed to the new light levels. The values of A and g_s were used to estimate iWUE (iWUE = A/g_s).

Monitoring electron transport and assimilation during light changes. A DUAL-PAM attached to a GFS-3000 (Walz) was used to monitor the responses of the effective photochemical quantum yield of PSII (F_q'/F_m') and PSI (Y(I)) and of A to changes in light intensity. To remove stomatal limitation of A, the plants were maintained at a constant temperature (24 °C), relative humidity (60%) and high CO_2 concentration (1,500 µmol mol^{-1}). The plants were dark adapted, and the induction/relaxation of the photosystems was tested by subjecting the plants to a step change in light intensity from 0 to 1,000 µmol m^{-2} s^{-1}; this intensity was maintained for 5 min before returning to dark.

Statistical analysis. All statistical analyses were done using Sys-stat (University of Essex) and R (RStudio v.1.1423, operating R v.3.6; https://www.r-project.org/). For the greenhouse and 2016 field experiment biomass data, seedling chlorophyll imaging and enzyme activities, analysis of variance (ANOVA) and post-hoc Tukey tests were done. For the gas-exchange curves, the data were compared by linear mixed model analysis using the lmer function and type III ANOVA[54]. Significant differences between manipulations were identified using contrasts analysis (lsmeans package). For the 2017 field experiments, the biomass data were compared by linear mixed model analysis using the lmer function and type III ANOVA to account for block effects using four plants per genotype for $n = 6$ blocks. For the analysis of electron transport and assimilation during light changes, the slopes of the activation curves were calculated for each parameter, and ANOVA and post-hoc Tukey tests were done.

Reporting Summary. Further information on research design is available in the Nature Research Reporting Summary linked to this article.

Data availability

The data that support the findings of this study, the plant transformation constructs and the seed are available from the corresponding authors on reasonable request.

Received: 8 January 2019; Accepted: 8 July 2020;
Published online: 10 August 2020

References

1. Zhu, X. G., Long, S. P. & Ort, D. R. Improving photosynthetic efficiency for greater yield. *Annu. Rev. Plant Biol.* **61**, 235–261 (2010).
2. Simkin, A. J., Lopez-Calcagno, P. E. & Raines, C. A. Feeding the world: improving photosynthetic efficiency for sustainable crop production. *J. Exp. Bot.* **70**, 1119–1140 (2019).
3. Simkin, A. J. Genetic engineering for global food security: photosynthesis and biofortification. *Plants* **8**, 586–615 (2019).
4. Miyagawa, Y., Tamoi, M. & Shigeoka, S. Overexpression of a cyanobacterial fructose-1,6-/sedoheptulose-1,7-bisphosphatase in tobacco enhances photosynthesis and growth. *Nat. Biotechnol.* **19**, 965–969 (2001).
5. Lefebvre, S. et al. Increased sedoheptulose-1,7-bisphosphatase activity in transgenic tobacco plants stimulates photosynthesis and growth from an early stage in development. *Plant Physiol.* **138**, 451–460 (2005).
6. Raines, C. A. Transgenic approaches to manipulate the environmental responses of the C_3 carbon fixation cycle. *Plant Cell Environ.* **29**, 331–339 (2006).
7. Rosenthal, D. M. et al. Over-expressing the C_3 photosynthesis cycle enzyme sedoheptulose-1-7 bisphosphatase improves photosynthetic carbon gain and yield under fully open air CO_2 fumigation (FACE). *BMC Plant Biol.* **11**, 123 (2011).
8. Simkin, A. J., McAusland, L., Headland, L. R., Lawson, T. & Raines, C. A. Multigene manipulation of photosynthetic carbon assimilation increases CO_2 fixation and biomass yield in tobacco. *J. Exp. Bot.* **66**, 4075–4090 (2015).
9. Simkin, A. J. et al. Simultaneous stimulation of sedoheptulose 1,7-bisphosphatase, fructose 1,6-bisphophate aldolase and the photorespiratory glycine decarboxylase-H protein increases CO_2 assimilation, vegetative biomass and seed yield in *Arabidopsis*. *Plant Biotechnol. J.* **15**, 805–816 (2017).
10. Zhu, X. G., de Sturler, E. & Long, S. P. Optimizing the distribution of resources between enzymes of carbon metabolism can dramatically increase photosynthetic rate: a numerical simulation using an evolutionary algorithm. *Plant Physiol.* **145**, 513–526 (2007).
11. Long, S. P., Zhu, X. G., Naidu, S. L. & Ort, D. R. Can improvement in photosynthesis increase crop yields? *Plant Cell Environ.* **29**, 315–330 (2006).
12. Poolman, M. G., Fell, D. A. & Thomas, S. Modelling photosynthesis and its control. *J. Exp. Bot.* **51**, 319–328 (2000).
13. Raines, C. A. The Calvin cycle revisited. *Photosynth. Res.* **75**, 1–10 (2003).
14. Uematsu, K., Suzuki, N., Iwamae, T., Inui, M. & Yukawa, H. Increased fructose 1,6-bisphosphate aldolase in plastids enhances growth and photosynthesis of tobacco plants. *J. Exp. Bot.* **63**, 3001–3009 (2012).
15. Ding, F., Wang, M. L., Zhang, S. X. & Ai, X. Z. Changes in SBPase activity influence photosynthetic capacity, growth, and tolerance to chilling stress in transgenic tomato plants. *Sci. Rep.* **6**, 32741 (2016).
16. Driever, S. M. et al. Increased SBPase activity improves photosynthesis and grain yield in wheat grown in greenhouse conditions. *Phil. Trans. R. Soc. B* **372**, 1730 (2017).

17. Tamoi, M., Nagaoka, M., Miyagawa, Y. & Shigeoka, S. Contribution of fructose-1,6-bisphosphatase and sedoheptulose-1,7-bisphosphatase to the photosynthetic rate and carbon flow in the Calvin cycle in transgenic plants. *Plant Cell Physiol.* **47**, 380–390 (2006).
18. Ichikawa, Y. et al. Generation of transplastomic lettuce with enhanced growth and high yield. *GM Crops* **1**, 322–326 (2010).
19. Kohler, I. H. et al. Expression of cyanobacterial FBP/SBPase in soybean prevents yield depression under future climate conditions. *J. Exp. Bot.* **68**, 715–726 (2017).
20. Simkin, A. J., McAusland, L., Lawson, T. & Raines, C. A. Overexpression of the Rieske FeS protein increases electron transport rates and biomass yield. *Plant Physiol.* **175**, 134–145 (2017).
21. Ermakova, M., Lopez-Calcagno, P. E., Raines, C. A., Furbank, R. T. & von Caemmerer, S. Overexpression of the Rieske FeS protein of the cytochrome b_6f complex increases C_4 photosynthesis in *Setaria viridis*. *Commun. Biol.* **2**, 314 (2019).
22. Chida, H. et al. Expression of the algal cytochrome c_6 gene in *Arabidopsis* enhances photosynthesis and growth. *Plant Cell Physiol.* **48**, 948–957 (2007).
23. Yadav, S. K., Khatri, K., Rathore, M. S. & Jha, B. Introgression of UfCyt c_6, a thylakoid lumen protein from a green seaweed *Ulva fasciata* Delile enhanced photosynthesis and growth in tobacco. *Mol. Biol. Rep.* **45**, 1745–1758 (2018).
24. Merchant, S. & Bogorad, L. The Cu(II)-repressible plastidic cytochrome *c*: cloning and sequence of a complementary DNA for the pre-apoprotein. *J. Biol. Chem.* **262**, 9062–9067 (1987).
25. De la Rosa, M. A., Molina-Heredia, F. P., Hervás, M. & Navarro, J. A. in *Photosystem I: Advances in Photosynthesis and Respiration* Vol. 24 (ed. Golbeck, J. H.) 683–696 (Springer, 2006).
26. Finazzi, G., Sommer, F. & Hippler, M. Release of oxidized plastocyanin from photosystem I limits electron transfer between photosystem I and cytochrome b6f complex in vivo. *Proc. Natl Acad. Sci. USA* **102**, 7031–7036 (2005).
27. Gong, H. Y. et al. Transgenic rice expressing Ictb and FBP/SBPase derived from cyanobacteria exhibits enhanced photosynthesis and mesophyll conductance to CO_2. *PLoS ONE* **10**, e0140928 (2015).
28. Wullschleger, S. D. Biochemical limitations to carbon assimilation in C_3 plants—a retrospective analysis of the A/Ci curves from 109 species. *J. Exp. Bot.* **44**, 907–920 (1993).
29. Pesaresi, P. et al. Mutants, overexpressors, and interactors of *Arabidopsis* plastocyanin isoforms: revised roles of plastocyanin in photosynthetic electron flow and thylakoid redox state. *Mol. Plant* **2**, 236–248 (2009).
30. López-Calcagno, P. E. et al. Overexpressing the H-protein of the glycine cleavage system increases biomass yield in glasshouse and field-grown transgenic tobacco plants. *Plant Biotechnol. J.* **17**, 141–151 (2018).
31. Glowacka, K. et al. Photosystem II subunit S overexpression increases the efficiency of water use in a field-grown crop. *Nat. Commun.* **9**, 868 (2018).
32. Busch, F. A. Opinion: the red-light response of stomatal movement is sensed by the redox state of the photosynthetic electron transport chain. *Photosynth. Res.* **119**, 131–140 (2014).
33. Engler, C., Gruetzner, R., Kandzia, R. & Marillonnet, S. Golden Gate shuffling: a one-pot DNA shuffling method based on type IIs restriction enzymes. *PLoS ONE* **4**, e5553 (2009).
34. Engler, C., Kandzia, R. & Marillonnet, S. A one pot, one step, precision cloning method with high throughput capability. *PLoS ONE* **3**, e3647 (2008).
35. Nakagawa, T. et al. Development of series of gateway binary vectors, pGWBs, for realizing efficient construction of fusion genes for plant transformation. *J. Biosci. Bioeng.* **104**, 34–41 (2007).
36. Simkin, A. J. et al. Characterization of the plastidial geraniol synthase from Madagascar periwinkle which initiates the monoterpenoid branch of the alkaloid pathway in internal phloem associated parenchyma. *Phytochemistry* **85**, 36–43 (2013).
37. Richins, R. D., Scholthof, H. B. & Shepherd, R. J. Sequence of figwort mosaic-virus DNA (*Caulimovirus* group). *Nucleic Acids Res.* **15**, 8451–8466 (1987).
38. Horsch, R. B., Rogers, S. G. & Fraley, R. T. Transgenic plants—technology and applications. *Abstr. Pap. Am. Chem. S.* **190**, 67 (1985).
39. Hoagland, D. R. & Arnon, D. I. *The Water-Culture Method for Growing Plants without Soil* (College of Agriculture, 1950).
40. Kromdijk, J. et al. Improving photosynthesis and crop productivity by accelerating recovery from photoprotection. *Science* **354**, 857–861 (2016).
41. Lopez-Calcagno, P. E., Abuzaid, A. O., Lawson, T. & Raines, C. A. *Arabidopsis* CP12 mutants have reduced levels of phosphoribulokinase and impaired function of the Calvin–Benson cycle. *J. Exp. Bot.* **68**, 2285–2298 (2017).
42. Dunford, R. P., Catley, M. A., Raines, C. A., Lloyd, J. C. & Dyer, T. A. Purification of active chloroplast sedoheptulose-1,7-bisphosphatase expressed in *Escherichia coli*. *Protein Expr. Purif.* **14**, 139–145 (1998).
43. Henkes, S., Sonnewald, U., Badur, R., Flachmann, R. & Stitt, M. A small decrease of plastid transketolase activity in antisense tobacco transformants has dramatic effects on photosynthesis and phenylpropanoid metabolism. *Plant Cell* **13**, 535–551 (2001).
44. Khozaei, M. et al. Overexpression of plastid transketolase in tobacco results in a thiamine auxotrophic phenotype. *Plant Cell* **27**, 432–447 (2015).
45. Hiyama, T. Isolation of photosystem I particles from spinach. *Methods Mol. Biol.* **274**, 11–17 (2004).
46. Zhao, Y. L. et al. Downregulation of transketolase activity is related to inhibition of hippocampal progenitor cell proliferation induced by thiamine deficiency. *Biomed. Res. Int.* **2014**, 572915 (2014).
47. Barbagallo, R. P., Oxborough, K., Pallett, K. E. & Baker, N. R. Rapid, noninvasive screening for perturbations of metabolism and plant growth using chlorophyll fluorescence imaging. *Plant Physiol.* **132**, 485–493 (2003).
48. von Caemmerer, S. et al. Stomatal conductance does not correlate with photosynthetic capacity in transgenic tobacco with reduced amounts of Rubisco. *J. Exp. Bot.* **55**, 1157–1166 (2004).
49. Baker, N. R., Oxborough, K., Lawson, T. & Morison, J. I. L. High resolution imaging of photosynthetic activities of tissues, cells and chloroplasts in leaves. *J. Exp. Bot.* **52**, 615–621 (2001).
50. Oxborough, K. & Baker, N. R. An evaluation of the potential triggers of photoinactivation of photosystem II in the context of a Stern–Volmer model for downregulation and the reversible radical pair equilibrium model. *Phil. Trans. R. Soc. Lond. B* **355**, 1489–1498 (2000).
51. Lawson, T., Lefebvre, S., Baker, N. R., Morison, J. I. L. & Raines, C. A. Reductions in mesophyll and guard cell photosynthesis impact on the control of stomatal responses to light and CO_2. *J. Exp. Bot.* **59**, 3609–3619 (2008).
52. Farquhar, G., von Caemmerer, S. V. & Berry, J. A biochemical model of photosynthetic CO_2 assimilation in leaves of C_3 species. *Planta* **149**, 78–90 (1980).
53. Sharkey, T. D., Bernacchi, C. J., Farquhar, G. D. & Singsaas, E. L. Fitting photosynthetic carbon dioxide response curves for C_3 leaves. *Plant Cell Environ.* **30**, 1035–1040 (2007).
54. Vialet-Chabrand, S., Matthews, J. S. A., Simkin, A. J., Raines, C. A. & Lawson, T. Importance of fluctuations in light on plant photosynthetic acclimation. *Plant Physiol.* **173**, 2163–2179 (2017).
55. von Caemmerer, S. & Farquhar, G. D. Some relationships between the biochemistry of photosynthesis and the gas-exchange of leaves. *Planta* **153**, 376–387 (1981).

Acknowledgements

This study was supported by the Realising Improved Photosynthetic Efficiency (RIPE) initiative awarded to C.A.R. by the University of Illinois. RIPE was possible through support from the Bill & Melinda Gates Foundation, DFID and FFAR, grant no. OPP1172157. This work was also supported by the Biotechnology and Biological Sciences Research Council (BBSRC) grant no. BB/J004138/1. We thank J. Matthews (University of Essex) for help with the data analysis, E. A. Pelech (University of Illinois) and S. Subramaniam (University of Essex) for help with plant growth, P. A. Davey (University of Essex) and R. Gossen (University of Helsinki) for help with gas exchange, and D. Drag, B. Harbaugh and the Ort lab (University of Illinois) for support with the field trials.

Author contributions

P.E.L.-C. and A.J.S. generated the transgenic plants. P.E.L.-C., A.J.S., K.L.B. and S.J.F. performed the molecular and biochemical experiments. P.E.L.-C., A.J.S. and K.L.B. carried out the plant phenotypic and growth analysis and performed the gas-exchange measurements. S.V.-C. made the measurements of photosynthesis during light induction. A.J.S. and S.J.F. performed the enzyme assays on selected lines. All authors carried out data analysis on their respective contributions. C.A.R. and T.L. designed and supervised the research. P.E.L.-C., A.J.S. and C.A.R. wrote the manuscript. T.L. contributed to the editing of the manuscript and finalizing of the figures.

Competing interests

The authors declare no competing interests.

Additional information

Supplementary information is available for this paper at https://doi.org/10.1038/s41477-020-0740-1.

Correspondence and requests for materials should be addressed to P.E.L.-C. or C.A.R.

Reprints and permissions information is available at www.nature.com/reprints.

Publisher's note Springer Nature remains neutral with regard to jurisdictional claims in published maps and institutional affiliations.

nature research

Corresponding author(s): Christine A. Raines

Last updated by author(s): 19/06/2020

Reporting Summary

Nature Research wishes to improve the reproducibility of the work that we publish. This form provides structure for consistency and transparency in reporting. For further information on Nature Research policies, see Authors & Referees and the Editorial Policy Checklist.

Statistics

For all statistical analyses, confirm that the following items are present in the figure legend, table legend, main text, or Methods section.

n/a	Confirmed	
☐	☒	The exact sample size (*n*) for each experimental group/condition, given as a discrete number and unit of measurement
☐	☒	A statement on whether measurements were taken from distinct samples or whether the same sample was measured repeatedly
☐	☒	The statistical test(s) used AND whether they are one- or two-sided *Only common tests should be described solely by name; describe more complex techniques in the Methods section.*
☒	☐	A description of all covariates tested
☒	☐	A description of any assumptions or corrections, such as tests of normality and adjustment for multiple comparisons
☐	☒	A full description of the statistical parameters including central tendency (e.g. means) or other basic estimates (e.g. regression coefficient) AND variation (e.g. standard deviation) or associated estimates of uncertainty (e.g. confidence intervals)
☐	☒	For null hypothesis testing, the test statistic (e.g. *F*, *t*, *r*) with confidence intervals, effect sizes, degrees of freedom and *P* value noted *Give P values as exact values whenever suitable.*
☒	☐	For Bayesian analysis, information on the choice of priors and Markov chain Monte Carlo settings
☒	☐	For hierarchical and complex designs, identification of the appropriate level for tests and full reporting of outcomes
☒	☐	Estimates of effect sizes (e.g. Cohen's *d*, Pearson's *r*), indicating how they were calculated

Our web collection on statistics for biologists contains articles on many of the points above.

Software and code

Policy information about availability of computer code

Data collection	Chlorophyll fluorescence parameters were obtained using a chlorophyll fluorescence (CF) imaging system (Technologica, Colchester, UK) regularly used and highly cited. Photosynthetic gas-exchange and chlorophyll fluorescence parameters were recorded using a portable infrared gas analyser (LI-COR 6400; LI-COR, Lincoln, NE, USA). These equipment and associated software is commercially available, regularly used and highly cited.
Data analysis	All statistical analyses were done using Sys-stat, University of Essex, UK, and R (https://www.r-project.org/). For harvest data, seedling chlorophyll imaging and enzyme activities, analysis of variance and Post hoc Tukey test were done. For gas exchange curves, data were compared by linear mixed model analysis using lmer function and type III anova. Significant differences between manipulations were identified using contrasts analysis (lsmeans package).

For manuscripts utilizing custom algorithms or software that are central to the research but not yet described in published literature, software must be made available to editors/reviewers. We strongly encourage code deposition in a community repository (e.g. GitHub). See the Nature Research guidelines for submitting code & software for further information.

Data

Policy information about availability of data

All manuscripts must include a data availability statement. This statement should provide the following information, where applicable:

- Accession codes, unique identifiers, or web links for publicly available datasets
- A list of figures that have associated raw data
- A description of any restrictions on data availability

The data that support the findings of this study, plant transformation constructs and seed are available from the corresponding authors on reasonable request.

Field-specific reporting

Please select the one below that is the best fit for your research. If you are not sure, read the appropriate sections before making your selection.

☒ Life sciences ☐ Behavioural & social sciences ☐ Ecological, evolutionary & environmental sciences

For a reference copy of the document with all sections, see nature.com/documents/nr-reporting-summary-flat.pdf

Life sciences study design

All studies must disclose on these points even when the disclosure is negative.

Sample size	Experiments were designed to allow enough replication within the capacity of the growing facilities and was based on previous experience of variability that occurs between and within the different plant genotypes (Wild type, Azygous and Transgenic) Greenhouse experiments contained 6 individuals per line and 2-4 lines per manipulation giving an n = or > 12 similarly, fluorescence screening of seedling was performed on 3-7 or more individuals per line, and 2-4 lines per manipulation giving an n = or > 6. Figure 2 Mature leaves CN (n=10), SB (n=7), C6 (n=11), SBC6 (n=9) cv. Petit Havana (b) mature leaves of CN (n=10), S (n=8), SC6 (n=10) and (c) developing leaves CN (n=6), S (n=6), SC6 (n=9) cv. Samsun. Figure 3 Petite Havana CN (n=17), SB (n=21), C6 (n=18), (SBC6 n=18); cv. Samsun CN (n= 16), S (n=7, SC6 (n= 13). In field experiments the sample size was 6 plants per line (2016) or up to 24 plants per line (2017), and 2-3 lines per manipulation. Figure 4 2016 Experiment CN (n=72), SB (n=33), C6 (n=33); 2017 Experiment 1: CN (n=93), SB (n=71), C6 (n=70); 2017 Experiment 2: (n=97), C6 (n=72), SBC6 (n=47) Mean ± SE presented. Figure 5 & 6 a) 2017 experiment 1: CN (n= 21), SB (n=16) and C6 (n=16). (b) 2017 experiment 2: Lines expressing cytochrome CN (n=22) C6 (n=16), SBC6 (n=14). Sample sizes were based on previous field work looking at variation across the field under different designs.
Data exclusions	No data was excluded
Replication	Field experiments were not replicated, although the same single manipulations were tested in different 2 years. Additionally, the 2017 experiments had a replicated randomised design. Controlled conditions experiments were replicated with similar results
Randomization	For glasshouse experiments, the plants were randomly positioned and moved 3 times a week. carefully avoiding positioning plants from the same manipulation next to each other. For the field Experiments: 2016: The experiment was designed with a replicated control design. Each row was 4x14 with the outer plant being a wild type border control. Two lines per row were planted in an alternating pattern. The controls for each transgenic construct were the two rows of controls either side of the transgenic row. 2017: The field design was randomized rows split into three blocks, where each one row has all 15 lines and one block had one line of each construct. Rows were randomized using RAND function, Microsoft Excel 2010. All physiological measurements were taken from a subset of the population which was also sampled for gene and protein expression.
Blinding	No blinding. Due to the experimental design the scientists were aware of the position/identity of each plant.

Reporting for specific materials, systems and methods

We require information from authors about some types of materials, experimental systems and methods used in many studies. Here, indicate whether each material, system or method listed is relevant to your study. If you are not sure if a list item applies to your research, read the appropriate section before selecting a response.

Materials & experimental systems

n/a	Involved in the study
☐	☒ Antibodies
☒	☐ Eukaryotic cell lines
☒	☐ Palaeontology
☒	☐ Animals and other organisms
☒	☐ Human research participants
☒	☐ Clinical data

Methods

n/a	Involved in the study
☒	☐ ChIP-seq
☒	☐ Flow cytometry
☒	☐ MRI-based neuroimaging

Antibodies

Antibodies used	primary antibodies used: SBPase, FBP/SBPase, transketolase and cytochrome c6, see below for details
Validation	SBPase and transketolase antibodies have been previously used and reported in the following publications: SBPase: Dunford et al., 1998, Protein Expr Purif. Lefebvre et al., 2005, Plant Physiol. Transketolase: Henkes et al., 2001, The Plant Cell. Khozaei et al., 2015, The Plant Cell.

FBP/SBPase antibodies and cytochrome c6 antibodies were raised against synthetic peptides, [C]-DRPRHKELIQEIRNAG-amide, and [C]-[Nle]-PDKTLKKDVLEANS-amide respectively (Cambridge Research Biochemicals, Cleveland, UK). Both of these antibodies were tested against WT plants (not expressing the target proteins) and transgenic plants. Additionally, the cytochrome c6 antibodies were tested against Porphyra sp. protein extract and against purified cytochrome c6 protein.